

## c-Kit modifies the inflammatory status of smooth muscle cells

Lei Song<sup>1</sup>, Laisel Martinez<sup>2</sup>, Zachary M Zigmund<sup>1</sup>, Diana R Hernandez<sup>2</sup>, Roberta M Lassance-Soares<sup>2</sup>, Guillermo Selman<sup>2</sup>, Roberto I Vazquez-Padron<sup>Corresp. 2</sup>

<sup>1</sup> Department of Molecular and Cellular Pharmacology, University of Miami, Miami, FL, United States

<sup>2</sup> Department of Surgery, University of Miami, Miami, FL, United States

Corresponding Author: Roberto I Vazquez-Padron  
Email address: rvazquez@med.miami.edu

**Background:** c-Kit is a receptor tyrosine kinase present in multiple cell types including vascular smooth muscle cells (SMC). However, little is known about how c-Kit influences SMC biology and vascular pathogenesis. **Methods:** High-throughput microarray assays and *in silico* pathway analysis were used to identify differentially expressed genes between primary c-Kit deficient (Kit<sup>W/W-v</sup>) and control (Kit<sup>+/+</sup>) SMC. Quantitative real-time RT-PCR and functional assays further confirmed the differences in gene expression and pro-inflammatory pathway regulation between both SMC populations. **Results:** The microarray analysis revealed elevated NF-κB gene expression secondary to the loss of c-Kit that affects both the canonical and alternative NF-κB pathways. Upon stimulation with an oxidized phospholipid as pro-inflammatory agent, c-Kit deficient SMC displayed enhanced NF-κB transcriptional activity, higher phosphorylated/total p65 ratio, and increased protein expression of NF-κB regulated pro-inflammatory mediators with respect to cells from control mice. The pro-inflammatory phenotype of mutant cells was ameliorated after restoring c-Kit activity using lentiviral transduction. Functional assays further demonstrated that c-Kit suppresses NF-κB activity in SMC in a TGFβ-activated kinase 1 (TAK1) and Nemo-like kinase (NLK) dependent manner. **Discussion:** Our study suggests a novel mechanism by which c-Kit suppresses NF-κB regulated pathways in SMC to prevent their pro-inflammatory transformation.

1           **c-Kit Modifies the Inflammatory Status of Smooth Muscle Cells**

2

3   Lei Song<sup>a</sup>, Laisel Martinez<sup>b</sup>, Zachary M. Zigmond<sup>a</sup>, Diana R. Hernandez<sup>b</sup>, Roberta M. Lassance-

4   Soares<sup>b</sup>, Guillermo Selman<sup>b</sup>, and Roberto I. Vazquez-Padron <sup>b,\*</sup>

5   <sup>a</sup> Molecular and Cellular Pharmacology Department, Leonard M. Miller School of Medicine,

6   University of Miami, Miami, FL 33136

7   <sup>b</sup> DeWitt Daughtry Family Department of Surgery, Division of Vascular Surgery, Leonard M.

8   Miller School of Medicine, University of Miami, Miami, FL 33136

9

10

11

12

13   **\* Corresponding Author:**

14   Roberto I. Vazquez-Padron, PhD

15   1600 NW 10th Ave, RMSB 1048

16   Miami, FL 33136, United States

17   Tel: (305) 243-1154

18   Fax: (305) 243-3134

19   Email: [RVazquez@med.miami.edu](mailto:RVazquez@med.miami.edu)

20 **ABSTRACT**

21           **Background:** c-Kit is a receptor tyrosine kinase present in multiple cell types including  
22 vascular smooth muscle cells (SMC). However, little is known about how c-Kit influences SMC  
23 biology and vascular pathogenesis. **Methods:** High-throughput microarray assays and *in silico*  
24 pathway analysis were used to identify differentially expressed genes between primary c-Kit  
25 deficient (Kit<sup>W/W-v</sup>) and control (Kit<sup>+/+</sup>) SMC. Quantitative real-time RT-PCR and functional  
26 assays further confirmed the differences in gene expression and pro-inflammatory pathway  
27 regulation between both SMC populations. **Results:** The microarray analysis revealed elevated  
28 NF-κB gene expression secondary to the loss of c-Kit that affects both the canonical and  
29 alternative NF-κB pathways. Upon stimulation with an oxidized phospholipid as pro-  
30 inflammatory agent, c-Kit deficient SMC displayed enhanced NF-κB transcriptional activity,  
31 higher phosphorylated/total p65 ratio, and increased protein expression of NF-κB regulated pro-  
32 inflammatory mediators with respect to cells from control mice. The pro-inflammatory  
33 phenotype of mutant cells was ameliorated after restoring c-Kit activity using lentiviral  
34 transduction. Functional assays further demonstrated that c-Kit suppresses NF-κB activity in  
35 SMC in a TGFβ-activated kinase 1 (TAK1) and Nemo-like kinase (NLK) dependent manner.  
36 **Discussion:** Our study suggests a novel mechanism by which c-Kit suppresses NF-κB regulated  
37 pathways in SMC to prevent their pro-inflammatory transformation.

38

39

40

41

## 42 INTRODUCTION

43           The c-Kit receptor tyrosine kinase is a proto-oncogene and stem cell marker that has been  
44 recently implicated in vascular pathogenesis. Widely recognized for its proliferative and anti-  
45 apoptotic role in hematopoietic stem and progenitor cells (Bernstein et al. 1991), c-Kit signaling  
46 is now known to increase endothelial permeability (Kim et al. 2014; Im et al. 2016), and regulate  
47 the phenotype of smooth muscle cells (SMC) in the vasculature (Wang et al. 2007; Davis et al.  
48 2009). On one hand, animal models indicate that c-Kit activation by its ligand the stem cell  
49 factor (SCF) plays an important role in the development of both arterial and venous intimal  
50 hyperplasia (IH) (Hollenbeck et al. 2004; Wang et al. 2006; Wang et al. 2007; Skartsis et al.  
51 2014). On the other hand, c-Kit expression preserves the SMC contractile phenotype (Davis et al.  
52 2009), and protects arteries from excessive atherosclerosis (Song et al. 2016). Therefore, whether  
53 c-Kit is beneficial or detrimental for the vasculature is still a matter of debate and warrants  
54 further investigations.

55           Expression of c-Kit and SCF in vascular myofibroblasts and SMC seems to be tightly  
56 regulated by a variety of physiological and pathological triggers. c-Kit positive SMC populate  
57 the intima of arteries and veins after vascular injury in models of angioplasty and vein grafting  
58 (Hollenbeck et al. 2004; Wang et al. 2006; Wang et al. 2007). Temporal upregulation of both c-  
59 Kit and SCF are reported after injury in these models (Hollenbeck et al. 2004; Wang et al. 2006;  
60 Wang et al. 2007), where c-Kit dependent induction of the Akt-Bcl-2 cascade is thought to  
61 mediate the anti-apoptotic and migratory SMC phenotype responsible for IH (Wang et al. 2007).  
62 The formation of venous IH in arteriovenous fistulas (AVF) also occurs secondary to the  
63 activation of c-Kit expressing adventitial progenitors and migration of c-Kit positive  
64 myofibroblasts to the intima (Skartsis et al. 2014). Both animal and human AVF demonstrate

65 higher numbers of c-Kit expressing SMC after surgery compared to preoperative veins, along  
66 with a transitional increase in SCF levels in animal models after AVF creation (Skartsis et al.  
67 2014).

68 A small population of c-Kit expressing myofibroblasts/SMC was also found in  
69 pulmonary arteries of patients with idiopathic pulmonary arterial hypertension but not in healthy  
70 controls (Montani et al. 2011). In line with this evidence, both SCF and c-Kit were upregulated  
71 in pulmonary arterioles of experimental animals with pulmonary hypertension, where c-Kit  
72 colocalized with cells in the endothelium, media and adventitia (Young et al. 2016). In the latter  
73 model, SCF/c-Kit signaling promotes pathological remodeling and pulmonary vascular cell  
74 proliferation after hypoxic stimulation via activation of the ERK1/2 pathway (Young et al.  
75 2016). Paradoxically, the presence of c-Kit in human primary pulmonary artery SMC upregulates  
76 the transcription factor myocardin and preserves the contractile SMC phenotype (Davis et al.  
77 2009), suggesting a protective role of c-Kit under certain vascular conditions.

78 Along with the upregulation of c-Kit, the above evidence indicates that SCF is expressed  
79 and released in the vasculature in response to different insults (Miyamoto et al. 1997; Hollenbeck  
80 et al. 2004; Wang et al. 2007). Vascular SCF exists in both membrane-bound and soluble forms,  
81 thus its ability to promote cell recruitment and elicit autocrine and paracrine responses, as well as  
82 cell-to-cell stimulation (Hollenbeck et al. 2004; Lennartsson and Ronnstrand 2012; Skartsis et al.  
83 2014). The soluble form of SCF is generated by alternative splicing or released through the  
84 proteolytic action of matrix metalloproteinase 9 (MMP-9) (Hollenbeck et al. 2004; Bengatta et al.  
85 2009; Lennartsson and Ronnstrand 2012; Klein et al. 2015). This latter enzyme is also  
86 upregulated in vascular remodeling processes, thereby perpetuating the local effects of the  
87 SCF/c-Kit pathway (Hollenbeck et al. 2004; Skartsis et al. 2014). Interestingly, the soluble and

88 membrane-bound SCF isoforms seem to have different effects on c-Kit activation (Miyazawa et  
89 al. 1995). The former causes rapid and transient stimulation and autophosphorylation of the  
90 receptor as well as fast degradation, whereas the latter leads to sustained activation (Miyazawa et  
91 al. 1995). This observation suggests that cell-to-cell interactions between SCF and c-Kit  
92 expressing SMC have the potential to significantly modify their respective phenotypes and  
93 nearby microenvironment. The concomitant expression of SCF and c-Kit in various cell types  
94 (Lennartsson and Ronnstrand 2006; Zakiryanova et al. 2014), including myofibroblasts/SMC  
95 (Hollenbeck et al. 2004; Wang et al. 2007; Skartsis et al. 2014), also implies the presence of an  
96 autocrine loop for the activation of this receptor. Unfortunately, the available data on the role of  
97 c-Kit in vascular remodeling processes is still scarce, and more information is particularly  
98 needed on the c-Kit mediated pathways that regulate the SMC phenotypic transformation (Wang  
99 et al. 2007).

100         In this work, we used high-throughput microarray analyses to identify differentially  
101 expressed genes as a result of c-Kit loss of function in arterial SMC isolated from mutant and  
102 littermate control mice. We combined *in silico* pathway analyses and confirmatory assays to  
103 further investigate the gene expression profiles of stimulated SMC under both experimental  
104 conditions. We showed increased NF- $\kappa$ B activation in c-Kit deficient SMC compared to their  
105 wild type counterparts. Furthermore, we demonstrated that these changes were associated with a  
106 heightened state of vascular inflammation, as indicated by the elevated protein expression of pro-  
107 inflammatory mediators in c-Kit deficient SMC. Outcomes from this study challenge the existing  
108 belief that vascular c-Kit expression is pathological and suggest instead a beneficial contribution  
109 of this signaling axis for the preservation of SMC's anti-inflammatory status under adverse  
110 conditions.

## 111 MATERIALS AND METHODS

### 112 *Smooth Muscle Cell Isolation and Culture*

113 Primary aortic SMC were isolated from c-Kit deficient ( $\text{Kit}^{\text{W/W-v}}$ ) mice and control  
114 littermate mice ( $\text{Kit}^{+/+}$ ) (Stock #100410, The Jackson Laboratories, Bar Harbor, ME) (Bernstein  
115 et al. 1990) using the explant technique (Metz et al. 2012) with minor modifications. Briefly,  
116 mouse aortas were digested with collagenase type II (5 mg/mL, Worthington, Lakewood, NJ) at  
117  $37^{\circ}\text{C}$  for 1 hour, after which they were transferred to 10% FBS and cut with a scalpel into small  
118 pieces. Individual SMC migrate out of the explants within 1 week of culture. Cells were  
119 maintained in DMEM-F12-FBS (5:3:2; Thermo Fisher Scientific, Waltham, MA) supplemented  
120 with 100  $\mu\text{g}/\text{ml}$  penicillin, 100  $\mu\text{g}/\text{ml}$  streptomycin, 0.1 mM glutamine, 10 mM sodium pyruvate,  
121 and 0.75% sodium bicarbonate (Metz et al. 2012). Primary cells were maintained at ~90%  
122 confluency and used within three passages to avoid fibroblast-like phenotypic switch. All animal  
123 procedures were performed according to the National Institutes of Health guidelines (Guide for  
124 the Care and Use of Laboratory Animals) and approved by the University of Miami Miller  
125 School of Medicine Institutional Animal Care and Use Committee (protocol 15-114).

### 126 *RNA Microarray and Pathway Analysis*

127 Total RNA was isolated from  $\text{Kit}^{+/+}$  and  $\text{Kit}^{\text{W/W-v}}$  SMC using the Quick-RNA MiniPrep  
128 kit (Zymo Research, Irvine, CA). RNA quality was validated in the Agilent 2100 Bioanalyzer  
129 (Agilent Technologies, Santa Clara, CA) before being sent to Ocean Ridge Biosciences (Palm  
130 Beach Gardens, FL) for Mouse MI-Ready Gene Expression Microarray analysis. Once in Ocean  
131 Ridge Biosciences, RNA processing included a 30-minute digestion with RNase-free DNase I  
132 (Epicentre, Madison, WI) at  $37^{\circ}\text{C}$  followed by purification using the AgenCourt RNAClean XP

133 bead method (Beckman Coulter, Indianapolis, IN). Biotin-labeled complementary RNA (cRNA)  
134 was prepared from 2  $\mu$ g per sample of re-purified RNA by the method of Van Gelder *et al.* (Van  
135 Gelder's Multi-gene expression profile - US Patent 7049102). Eighteen micrograms of  
136 biotinylated cRNA per sample were fragmented, diluted in formamide-containing hybridization  
137 buffer, and loaded onto the surface of the Mouse MI-Ready microarray slides enclosed in custom  
138 hybridization chambers. The slides were hybridized for 16-18 hours under constant rotation in a  
139 Model 400 hybridization oven (Scigene, Sunnyvale, CA). After hybridization, the microarray  
140 slides were washed under stringent conditions, stained with Streptavidin-Alexa-647 (Life  
141 Technologies, Waltham, MA), and scanned using an Axon GenePix 4000B scanner (Molecular  
142 Devices, Sunnyvale, CA). Probe intensities were calculated for each feature on each microarray  
143 by subtracting the median local background from the median local foreground for each probe.  
144 Data for all manufacturer-flagged probes and visually flagged probes impacting >25% of  
145 samples were removed. Data for visually flagged probes impacting < 25% of samples were  
146 replaced with the sample average for the probe. Probe intensities were transformed by taking the  
147 base 2 logarithm of each value. Array-specific detection thresholds (T) were calculated by  
148 adding 3 times the standard deviation of the median local background and the mean negative  
149 control probe signal. Probe intensity and T were normalized by subtracting the 70th percentile of  
150 the mouse probe intensities and adding back the mean of the 70th percentile across all samples as  
151 a scaling factor. The data were filtered to select for mouse probes showing signal above the  
152 normalized T in at least 25% of the samples; data for control sequences and other non-mouse  
153 probes were removed. Mouse probe sequences were annotated using a BLAST analysis of the  
154 Ensembl Mouse cDNA database version 84 (2016). Gene expression differences between Kit<sup>+/+</sup>  
155 and Kit<sup>W/W-v</sup> SMC were considered statistically significant if  $p < 0.05$  by *t-test*.

156 For pathway analysis, genes with statistically significant expression differences in  
157 microarray analysis were imported into the Ingenuity Pathway Analysis software  
158 (www.ingenuity.com; Ingenuity Systems, Redwood City, CA). The Core Analysis was used to  
159 identify the canonical pathways associated with the differentially expressed genes. Pathway  
160 overlap and p-value calculations were performed using the reference gene set in the Ingenuity  
161 Knowledge Base, where only molecular relationships (direct and indirect) that have been  
162 experimentally observed were considered. The Molecule Activity Predictor tool was used to  
163 estimate activation or inhibition of pathway branches based on the observed gene expression fold  
164 changes in Kit<sup>W/W-v</sup> vs. Kit<sup>+/+</sup> SMC.

#### 165 ***Quantitative Real-Time PCR (qPCR)***

166 Relative gene expression of selected mRNA transcripts was evaluated using TaqMan  
167 Gene Expression Assays (Applied Biosystems, Foster City, CA). Total RNA was isolated as  
168 described above, and cDNA synthesized with the High-Capacity cDNA Reverse Transcription  
169 kit (Applied Biosystems). Real-time RT-PCR was performed on an ABI Prism 7500 Fast Real-  
170 Time PCR System (96-well plate) (Applied Biosystems) using primers/probe sets  
171 complementary to the genes of interest (*ActB*, Mm00607939\_m1; *Ccl2*, Mm00441242\_m1;  
172 *Ikbka*, Mm00432529\_m1; *Ikbkb*, Mm01222247\_m1; *Ikbkg*, Mm00494927\_m1; *Il6*,  
173 Mm00446190\_m1; *Kit*, Mm00445212\_m1; *Kitl*, Mm00442972\_m1; *Map3k14*,  
174 Mm0048444166\_m1; *Mmp2*, Mm00439498\_m1; *Mmp9*, Mm00442991\_m1; *Nfkb2*,  
175 Mm00479807\_m1; *Nfkbia*, Mm00477798\_m1; *Nos2*, Mm00440502\_m1; *Ptgs2*,  
176 Mm00478374\_m1; *RelB*, Mm00485664-m1; *Tnf*, Mm00443258\_m1). Relative gene expression

177 was determined using the  $\Delta\Delta\text{CT}$  method (Livak and Schmittgen 2001) and normalized with  
178 respect to *ActB*.

### 179 ***Gene Rescue and Knockdown***

180 Gene rescue in c-Kit deficient ( $\text{Kit}^{\text{W/W}^v}$ ) SMC was performed using a lentiviral vector  
181 (pRVPG24). This rescue vector was constructed by inserting a blunted BsrBI-NotI digested  
182 DNA fragment (3.6 Kb), containing the coding region of the mouse Kit cDNA under the murine  
183 phosphoglycerate kinase (PGK) promoter, into the blunted EcoRV-ClaI digested pLenti CMV  
184 PuroDest vector (Addgene Inc., Cambridge, MA). Third generation lentiviral stocks were  
185 produced in HEK-293 cells co-transfected with the lentiviral vector and the packaging and  
186 envelope plasmids psPAX2 and pMD2.G (Addgene Inc.). Transfections were done with the  
187 jetPRIME transfection kit (Polyplus, New York, NY). Infected cells (100 MOI) were selected in  
188 DMEM-F12-FBS (5:3:2; Thermo Fisher Scientific) supplemented with 100  $\mu\text{g/ml}$  penicillin, 100  
189  $\mu\text{g/ml}$  streptomycin, 0.1 mM glutamine, 10 mM sodium pyruvate, 0.75% sodium bicarbonate,  
190 and 10  $\mu\text{g/ml}$  puromycin (Sigma, St Louis, MO).

191 Knockdown of TAK1 or NLK in c-Kit wild type ( $\text{Kit}^{+/+}$ ) SMC was performed using  
192 pooled lentiviral particles carrying different target siRNAs (Supplementary Table 1; Applied  
193 Biological Materials, Richmond, Canada). An anti-GFP siRNA was used as control. Transduced  
194 cells were puromycin-selected as described above. All gene modifications were confirmed by  
195 analytical flow cytometry or Western blot (WB).

196

197

198 *Flow Cytometry Analysis*

199 c-Kit surface expression was evaluated by flow cytometry in SMC stained with an anti-  
200 CD117 antibody (CD117-PE, Cat# 130-091730, Miltenyi Biotec, San Diego, CA). Analytical  
201 flow cytometry was performed on a BD FACS Canto II (BD Biosciences, San Jose, CA) using  
202 the BD FACSDiva software (Becton Dickinson, Franklin Lakes, NJ). Data were analyzed using  
203 the FlowJo software (Ashland, OR).

204 *Western Blot and Immunoprecipitation (IP)*

205 Whole cell protein lysates were prepared in RIPA buffer supplemented with 200 mM  
206 phenylmethylsulfonyl fluoride (PMSF), 100mM sodium orthovanadate (Santa Cruz  
207 Biotechnology, Dallas, TX), and a complete protease inhibitor cocktail (Roche Life Science,  
208 Indianapolis, IN). Lysate concentration was determined using a commercial Bradford's protein  
209 assay kit (BioRad, Hercules, CA). For WB analysis, ~50 µg of sample was loaded into a  
210 NuPAGE 4-12% Bis-Tris SDS-polyacrylamide gel (Thermo Fisher Scientific) and subsequently  
211 transferred to a PVDF membrane (GE Healthcare, Marlborough, MA). Specific proteins were  
212 detected using antibodies against c-Kit (1:1000, Cat# sc-1494, Santa Cruz Biotechnology), MCP-  
213 1, MMP-2, TAK1 (1:500, Cat# sc-1785, sc-1839, and sc-6838, Santa Cruz Biotechnology), NLK  
214 (1:1000, Cat# ab26050, Abcam, San Francisco, CA), Src (1:500, Cat# 2108S, Cell Signaling  
215 Technology, Danvers, MA), and  $\beta$ -Actin (1:5000, Cat# A5316, Sigma). Bound antibodies were  
216 detected after sequentially incubating the membranes with HRP-conjugated secondary  
217 antibodies. The Amersham ECL Western Blotting Detection Reagent (GE Healthcare) or  
218 SuperSignal West Femto Maximum Sensitivity Substrate Reagent (Thermo Fisher Scientific)  
219 were used for signal detection. Images were analyzed using ImageJ Pro 5.0.

220 For co-IP, ~200 µg of protein lysate was incubated at 4°C for 4 hours with 1 µg of anti- c-  
221 Kit (Cat# A4502, Dako, Santa Clara, CA) or TAK1 antibodies and 20 µl of Protein A/G PLUS-  
222 Agarose microbeads (Santa Cruz Biotechnologies). Microbeads were washed with cold RIPA  
223 buffer before WB analysis for c-Kit, TAK1, or NLK as indicated above.

#### 224 ***NF-κB Promoter Activity***

225 Primary SMC were transfected with a commercial mix of NF-κB Luc-reporter plasmids  
226 (Qiagen, Germantown, MD) using the Axama Basic Nucleofector Primary Smooth Muscle Cells  
227 electroporation kit (Cat# VPI-1004, Lonza, Walkersville, MD). Transfected cells were incubated  
228 with 1-palmitoyl-2-(5-oxovaleroyl)-sn-glycero-3-phosphocholine (POVPC; Avanti Polar Lipids,  
229 Alabaster, AL) for 24 hours in serum-free medium as previously described (Pidkovka et al.  
230 2007) before lysis using the Passive Lysis Buffer (Promega, Madison, WI). NF-κB promoter  
231 activity was determined using the Dual-Luciferase Reporter Assay System (Cat# E1910,  
232 Promega) in a Turner Biosystems Luminometer model Glomax 20/20 (Mountain View, CA), and  
233 normalized to the Renilla luciferase activity of the kit's internal control. Promoter activity was  
234 expressed as folds of control activity.

#### 235 ***Enzyme-Linked Immunosorbent Assay (ELISA)***

236 The levels of cellular NF-κB p65 and phosphorylated protein (p-p65) were measured in  
237 SMC treated with POVPC as described above. Cells were lysed using the 1X Cell Extraction  
238 Buffer PTR provided in the ELISA kit (Abcam, Cambridge, MA). The ELISA was performed  
239 using the NF-κB p65 (pS536 + Total) SimpleStep Kit (Abcam) following the manufacturer's

240 protocol. Protein levels were measured using an endpoint reading at OD 455 nm in an Ultramark  
241 Microplate Reader (BioRad).

## 242 *Statistics*

243 Results are presented as mean  $\pm$  standard deviation. A two-tailed student *t-test* was used  
244 to compare the difference between two groups, and one-way ANOVA followed by a Newman-  
245 Keuls test was applied to compare the difference among multiple groups. A *p* value  $<0.05$  was  
246 considered significant.

247

## 248 **RESULTS**

### 249 *Different gene expression profiles in c-Kit positive and deficient smooth muscle cells*

250 Considering the reported contribution of c-Kit to vascular remodeling processes  
251 (Hollenbeck et al. 2004; Wang et al. 2006; Wang et al. 2007; Skartsis et al. 2014; Young et al.  
252 2016), we sought for differentially expressed genes between primary SMC isolated from c-Kit  
253 deficient ( $\text{Kit}^{\text{W/W-v}}$ ) and control littermate ( $\text{Kit}^{+/+}$ ) mice (n=3 per strain). Out of a total of 34,265  
254 mouse probes queried by microarray, 18,224 yielded a detectable signal above threshold and  
255 1,086 genes were found differentially expressed between SMC from both experimental groups  
256 ( $p < 0.05$ ) (Figure 1A-B). Specifically, 564 and 522 transcripts were significantly up- and  
257 downregulated, respectively, with the loss of c-Kit activity with respect to control SMC (Figure  
258 1A). No statistically significant differences in expression were detected by microarray in the  
259 remaining 17,138 genes.

260 Table 1 presents selected differentially expressed genes in c-Kit deficient SMC that are  
261 relevant for inflammation such as *Ilf2*, *Ifna14*, and *Tnfsf9* (Zhao et al. 2005; Chan et al. 2006;  
262 Croft 2009). We also show decreased expression of the anti-inflammatory genes *Foxo1*, *Gdf6*,  
263 *Igf1*, *Igf2r*, and *Lpl* (Ziouzenkova et al. 2003; Sukhanov et al. 2007; Savai et al. 2014; Hisamatsu  
264 et al. 2016). Lipoprotein lipase (*Lpl*), for example, is 14-fold lower in c-Kit deficient cells than in  
265 those isolated from littermate controls. Additional changes in c-Kit deficient SMC are associated  
266 with a downregulation of the contractile SMC phenotype (increased *Tnfaip3* and reduced *Sirt1*)  
267 (Damrauer et al. 2010; Huang et al. 2015) and higher susceptibility to calcification (decreased  
268 *Foxo1* and *Pth1r*) (Cheng et al. 2010; Deng et al. 2015). Finally, we found significant  
269 expression differences in genes that code for cell adhesion proteins and for receptors and  
270 enzymes that regulate vasomotor responses (Table 1).

271 Confirmatory real-time RT-PCR assays were performed for selected inflammation-  
272 related genes that showed a trend by microarray analysis. Tumor necrosis factor (*Tnf*),  
273 interleukin 6 (*Il6*), C-C motif chemokine ligand 2 (*Ccl2*), metalloproteinases 2 and 9 (*Mmp2*,  
274 *Mmp9*), inducible nitric oxide synthase (*Nos2*), and cyclooxygenase 2 (*Ptgs2*) were significantly  
275 upregulated in c-Kit deficient SMC compared to controls (Figure 1C).

#### 276 ***Predicted activation of NF- $\kappa$ B signaling in c-Kit deficient cells by pathway analysis***

277 *In silico* pathway analysis was used to predict the molecular pathways affected by the  
278 loss of c-Kit in SMC. A total of 71 statistically significant pathways were identified ( $p < 0.05$ ) by  
279 the software, 42 of which with a biologically relevant function in SMC. These pathways covered  
280 cellular processes such as cell survival and apoptosis, inflammation, cell adhesion, nitric oxide  
281 signaling, and lipid metabolism (Table 2). Interestingly, 10 independent molecular pathways  
282 were associated with NF- $\kappa$ B signaling, and all of them showed either predicted activation of the

283 entire pathway (5/10; z-scores ranging from 0.258 to 1.265) or of the NF- $\kappa$ B branch (5/10) in c-  
284 Kit deficient SMC (Table 2).

### 285 ***Upregulation of NF- $\kappa$ B pathway genes in c-Kit deficient smooth muscle cells***

286 The NF- $\kappa$ B pathway plays a fundamental role in SMC differentiation, inflammation, and  
287 response to stress signals (Zahradka et al. 2002; Ramana et al. 2004; Mehrhof et al. 2005; Mack  
288 2011). Therefore, we confirmed the upregulation of components of this pathway in c-Kit  
289 deficient cells by real-time RT-PCR (Figure 1D). We found significantly higher expression  
290 levels of genes that are part of both the canonical (*Ikbka*, *Ikbkb*, *Ikbkg*, *Nfkbia*) and alternative  
291 (*Ikbka*, *Map3k14*, *Nfkb2*, *RelB*) NF- $\kappa$ B signaling pathways in Kit<sup>W/W-v</sup> vs. Kit<sup>+/+</sup> SMC.

### 292 ***Increased activity of the canonical NF- $\kappa$ B pathway in stimulated c-Kit deficient cells***

293 Given that the inhibitor of the canonical NF- $\kappa$ B pathway (*Nfkbia*) and the negative  
294 regulator *Tnfaip3* are upregulated in c-Kit deficient SMC (Table 1, Figure 1D), we turned to  
295 demonstrate the relationship between c-Kit expression and functional activity of the NF- $\kappa$ B  
296 signaling pathway. To further validate our findings, we rescued c-Kit expression in Kit<sup>W/W-v</sup>  
297 SMC by lentiviral transduction (Supplementary Figure 1).

298 POVPC-stimulated SMC with deficient c-Kit expression showed higher NF- $\kappa$ B  
299 transcriptional activity compared to wild type and c-Kit rescued cells as determined by a dual  
300 luciferase reporter assay (Figure 2A). Accordingly, a significantly higher ratio of the S536-  
301 phosphorylated/total p65 factor was detected in Kit<sup>W/W-v</sup> SMC vs. wild type and rescued cells  
302 (Figure 2B), demonstrating increased availability of active p65 in c-Kit deficient SMC for  
303 nuclear translocation and promoter binding (Lawrence 2009). Finally, we evaluated the protein  
304 concentrations of the pro-inflammatory mediators MMP-2 and MCP-1 in POVPC-stimulated

305 SMC, two factors that are regulated by NF- $\kappa$ B (Lee et al. 2008; Song et al. 2016). In agreement  
306 with the enhanced transcriptional activity shown above, the protein expressions of both MMP-2  
307 and MCP-1 were significantly higher in Kit<sup>W/W-v</sup> SMC compared to wild type and rescued cells  
308 (Figure 2C). To control for off-target effects of POVPC stimulation on c-Kit expression, we  
309 demonstrated that this treatment did not modify the cellular levels of SCF or the receptor  
310 (Supplementary Figure 2).

### 311 ***c-Kit regulates NF- $\kappa$ B activation through TAK1/NLK in smooth muscle cells***

312 Previous studies indicate an association between c-Kit, Lyn (a member of the Src family  
313 of non-receptor tyrosine kinases), and TAK1 (Drube et al. 2015), a negative regulator of NF- $\kappa$ B  
314 signaling (Ajibade et al. 2012). Therefore, we assessed whether this latter factor or its  
315 downstream partner NLK (Yasuda et al. 2004; Li et al. 2014) were responsible for the observed  
316 inhibition of the NF- $\kappa$ B pathway in c-Kit expressing SMC. We found that the protein  
317 expressions of both TAK1 and NLK were reduced or lost in Kit<sup>W/W-v</sup> SMC compared to wild  
318 type or c-Kit rescued cells (Figure 3A). Next, we selectively knocked down TAK1 or NLK in  
319 Kit<sup>+/+</sup> SMC (Figure 3B-C), and showed that this genetic manipulation restored the NF- $\kappa$ B  
320 transcriptional activity, phosphorylated/total p65 ratio, and protein expressions of MMP-2 and  
321 MCP1 in POVPC-stimulated c-Kit wild type SMC (Figure 3D-F). Lastly, we demonstrated by  
322 co-IP a physical interaction between all c-Kit, Src, TAK1, and NLK (Figure 4), further  
323 supporting a direct relationship in NF- $\kappa$ B regulation. Altogether, these experiments demonstrate  
324 that c-Kit inhibits NF- $\kappa$ B signaling in SMC through the actions of TAK1 and NLK.

325

326

327 **DISCUSSION**

328           Vascular SMC are characterized by tremendous phenotypic diversity (Yoshida and  
329 Owens 2005). Moreover, their contribution to vascular pathogenesis greatly depends on their  
330 phenotype and state of differentiation (Archer 1996; Yoshida and Owens 2005). Expression of  
331 the c-Kit receptor in SMC has been associated with various vascular pathologies in both animal  
332 models (Wang et al. 2006; Wang et al. 2007; Skartsis et al. 2014; Young et al. 2016) and human  
333 samples (Hollenbeck et al. 2004; Skartsis et al. 2014). In contrast, it has also proven protective in  
334 models of atherosclerosis (Song et al. 2016). In light of this evidence, there is little information  
335 on how c-Kit influences the phenotypes of SMC or the mechanisms by which they contribute to  
336 pathology. Our work reveals that the absence of c-Kit modified the expression of approximately  
337 6% of the genes that were detected by microarray in SMC from c-Kit mutant and littermate  
338 control mice. Furthermore, we provide evidence that c-Kit suppresses NF- $\kappa$ B signaling in SMC  
339 and decreases the production of pro-inflammatory mediators under stimulus.

340           Using *in silico* pathway analysis, we first demonstrated that c-Kit signaling influences a  
341 wide variety of cellular processes in SMC. Specifically, we found evidence of a pro-synthetic  
342 and pro-inflammatory phenotype in SMC secondary to the loss of this receptor. This is  
343 particularly evident by the potential dysregulation of lipid metabolism as indicated by a 14-fold  
344 decrease in *Lpl* gene expression. While increased vascular lipoprotein lipase can be pro-  
345 atherogenic (Clee et al. 2000), it is also believed to have anti-inflammatory properties both by  
346 generating metabolic PPAR agonists and inhibiting NF- $\kappa$ B activity (Ziouzenkova et al. 2003;  
347 Kota et al. 2005). c-Kit deficient cells also have decreased expression of the anti-inflammatory  
348 and anti-atherogenic factor IGF-1 (Sukhanov et al. 2007) and increased susceptibility to  
349 calcification due to the downregulation of the *Foxo1* and *Pth1r* genes (Cheng et al. 2010; Deng

350 et al. 2015). It is possible that these changes explain the increased severity of atherosclerosis in  
351 c-Kit mutant animals (Song et al. 2016). In addition, c-Kit deficient SMC appear to respond  
352 differently to vasomotor stimuli. Their gene expression profile indicates a significantly lower  
353 expression of vasoconstrictive G-protein coupled receptors such as the angiotensin II receptor  
354 type 1B and the arginine vasopressin receptor 1A. The response to nitric oxide may be also  
355 impaired in these cells due to a lower expression of guanylate cyclase 1 soluble subunit beta and  
356 cGMP-dependent protein-kinase type I. In the absence of functional experiments, it is not clear  
357 what is the biological impact of the above differences in c-Kit deficient SMC compared to their  
358 wild type counterparts. However, these observations warrant further investigations.

359         Interestingly, 24% of the differentially regulated pathways identified were associated  
360 with NF- $\kappa$ B signaling. Furthermore, both the *in silico* analysis and our experimental data  
361 demonstrated activation of this pathway in c-Kit deficient SMC with respect to those from  
362 littermate controls. NF- $\kappa$ B signaling is critical for the regulation of proliferation, differentiation,  
363 stress responses, and inflammatory processes in vascular SMC (Zahradka et al. 2002; Ramana et  
364 al. 2004; Mehrhof et al. 2005; Mack 2011). Whether NF- $\kappa$ B activation is associated with  
365 increased proliferation or apoptosis in SMC is dependent on the upstream stimuli and the type of  
366 vessel (Zahradka et al. 2002; Mehrhof et al. 2005; Ogbozor et al. 2015). A recent study  
367 demonstrated that NF- $\kappa$ B activation led to increased proliferation in fibroblasts, while inducing  
368 apoptosis and inflammation in SMC (Mehrhof et al. 2005). On the other hand, NF- $\kappa$ B was shown  
369 to be an important intracellular mediator of angiotensin II responses, leading to SMC  
370 proliferation and migration under these conditions (Zahradka et al. 2002). In terms of cell  
371 differentiation, NF- $\kappa$ B is known to repress myocardin activity and cause downregulation of SMC  
372 contractile genes (Tang et al. 2008). This molecular interaction has been implicated in the origin

373 of synthetic SMC under inflammatory processes such as atherosclerosis (Mack 2011).  
374 Interestingly, the reduced expression of *Sirt* and increased mRNA level of *Tnfaip3* in c-Kit  
375 deficient cells are independently associated with downregulation of contractile genes in SMC  
376 (Damrauer et al. 2010; Huang et al. 2015). These observations are in agreement with the  
377 predicted de-differentiated phenotype of c-Kit deficient SMC (Davis et al. 2009) and with the  
378 reported atheroprotective role of the c-Kit receptor (Song et al. 2016). TNFAIP3 normally  
379 provides a negative regulatory loop for the NF- $\kappa$ B pathway, including the decreased downstream  
380 production of the MCP-1 inflammatory mediator (Patel et al. 2006; Giordano et al. 2014).  
381 Downregulation of the *Crebbp* transcription factor is also thought to reduce NF- $\kappa$ B  
382 transcriptional activity (Yang et al. 2010). Nonetheless, neither higher *Tnfaip3* expression nor  
383 less *Crebbp* in c-Kit deficient SMC seem to have an appreciable inhibitory effect on NF- $\kappa$ B  
384 signaling, as demonstrated by our functional experiments and the increased protein expressions  
385 of the MMP-2 and MCP-1 factors.

386       Typical stimuli for NF- $\kappa$ B activation include cytokines, endotoxins, lipids, and  
387 mechanical stress (Maziere et al. 1996; De Martin et al. 2000; Kumar and Boriek 2003). For  
388 example, the oxidized phospholipid POVPC has been previously used to induce inflammation in  
389 vascular SMC (Pidkovka et al. 2007; Lu et al. 2013) and NF- $\kappa$ B activation (Pegorier et al. 2006;  
390 Vladykovskaya et al. 2011; Lu et al. 2013). As predicted by the *in silico* analysis, c-Kit  
391 deficiency in SMC led to higher levels of NF- $\kappa$ B transcriptional activity, phosphorylation of its  
392 key subunit p65, and expression of the NF- $\kappa$ B regulated inflammatory mediators MMP-2 and  
393 MCP-1 under POVPC challenge. Gene members of the non-canonical NF- $\kappa$ B pathway and other  
394 inflammatory mediators were also upregulated in mutant SMC.

395           The role of c-Kit as a negative regulator of the NF- $\kappa$ B pathway and related inflammation  
396 has been previously observed in other cell types and under different stimuli (Jin et al. 2013;  
397 Micheva-Viteva et al. 2013). Pharmacological inhibition of c-Kit results in increased activation  
398 of NF- $\kappa$ B in HEK293 cells and secretion of TNF $\alpha$  in dendritic cells and the THP-1 monocytic  
399 cell line in response to bacterial infection (Micheva-Viteva et al. 2013). Lower expressions of  
400 SCF and c-Kit were also associated with increased NF- $\kappa$ B signaling and oxidative stress in  
401 gastric smooth muscle (Jin et al. 2013).

402           Our experiments further revealed that c-Kit reduces NF- $\kappa$ B mediated inflammation via a  
403 direct molecular interaction with the NF- $\kappa$ B negative regulators TAK1 and NLK (Yasuda et al.  
404 2004; Ajibade et al. 2012; Li et al. 2014). The physical association between c-Kit, Lyn (a  
405 member of the Src family of non-receptor tyrosine kinases), and TAK1 has been previously  
406 observed in the HEK293T cell line, where these proteins form a signalosome that interacts with  
407 IKK $\beta$ , one of the catalytic units of the I $\kappa$ B kinase (IKK) complex (Drube et al. 2015).  
408 Nonetheless, the inhibitory activity of TAK1 on the NF- $\kappa$ B signaling pathway appears to be cell-  
409 specific, since in some cells it can be activating (Israel 2010; Ajibade et al. 2012). In the  
410 inhibitory instances, TAK1 blocks the phosphorylation and inactivates IKK (Ajibade et al.  
411 2012), which in turn is unable to phosphorylate and induce proteosomal degradation of the I $\kappa$ B  
412 inhibitors of the NF- $\kappa$ B pathway (Karin 1999; Israel 2010). When active, I $\kappa$ B proteins prevent  
413 the nuclear translocation of p65/RelA complexes (Karin 1999; Israel 2010). NLK also functions  
414 as an inhibitor of IKK phosphorylation (even in cells where TAK1 acts as an activator) (Li et al.  
415 2014). Therefore, our data indicate that in SMC the roles of TAK1 and NLK may be redundant.

416           In conclusions, our study demonstrates that c-Kit expression in SMC has an anti-  
417 inflammatory role. Our mechanistic studies contradict the existing belief about the noxious effect

418 of SCF/c-Kit signaling to the vasculature. It is noteworthy to recognize that such idea originated  
419 from descriptive studies and models of post injury IH. The current knowledge describes the  
420 expression of SCF and its receptor c-Kit in endothelial cells and SMC (Hollenbeck et al. 2004;  
421 Matsui et al. 2004; Wang et al. 2007; Skartsis et al. 2014), and suggests a key role for this  
422 signaling pathway in myofibroblast mobilization towards the neointima (Hollenbeck et al. 2004;  
423 Skartsis et al. 2014). Increased survival of SCF-treated SMC through Akt has also been  
424 demonstrated (Wang et al. 2007). In contrast, one recent study revealed that SCF/c-Kit signaling  
425 protects hyperlipidemic ApoE<sup>-/-</sup> mice from excessive atherosclerotic plaque deposition (Song et  
426 al. 2016). This apparent discrepancy may reflect the existing differences between IH (restenosis)  
427 and atherosclerosis in terms of etiology, natural history, culprit lesions, and progenitor cell  
428 contribution to disease progression. Therefore, our results suggests that while c-Kit positive cells  
429 have a detrimental effect on proliferative vascular lesions, their presence may prove protective in  
430 inflammatory conditions such as atherosclerosis. In addition, we propose a novel pathway for  
431 NF- $\kappa$ B regulation downstream of c-Kit activation. This information could be relevant in the  
432 setting of atherosclerosis disease development and complications, and may shed light on new  
433 proliferation control mechanisms to address IH after vascular injury.

434 **FIGURE LEGENDS**435 **Figure 1. Loss of c-Kit function accounts for significant gene expression differences**436 **between c-Kit deficient and wild type smooth muscle cells (SMC). A)** Venn diagram

437 indicating the numbers of differentially upregulated genes in primary SMC isolated from c-Kit

438 deficient (blue;  $Kit^{W/W-v}$ ) and littermate control mice (red;  $Kit^{+/+}$ ) as determined by microarray

439 analysis. The group of genes in the interception (black area) did not show statistically significant

440 differences by *t-test* between the two strains (n=3 per group). **B)** Heat map of differentially441 expressed genes in primary SMC from c-Kit deficient and littermate control mice. **C-D)** Relative442 expression of inflammatory **(C)** and NF- $\kappa$ B related **(D)** genes in c-Kit deficient vs. control SMC443 as determined by real-time RT-PCR. Values are shown as fold change over expression in  $Kit^{+/+}$ 444 cells; \*  $p < 0.05$  and \*\*  $p < 0.01$  using a two-tailed *t-test* assuming unequal variance, n=3 per

445 group.

446 **Figure 2. Loss of c-Kit function in primary smooth muscle cells (SMC) is associated with**447 **increased NF- $\kappa$ B activity. A)** NF- $\kappa$ B transcriptional activity in c-Kit deficient ( $Kit^{W/W-v}$ ),448 control ( $Kit^{+/+}$ ), and c-Kit rescued SMC ( $Kit^R$ ) after 24-hour treatment with POVPC (50  $\mu$ g/ml),

449 as determined by dual-luciferase reporter assay. Transcriptional activity is represented as the

450 mean  $\pm$  standard deviation (SD) of the Firefly/Renilla luciferase ratio normalized with respect to451 the control group ( $Kit^{+/+}$ ) (n=3 independent experiments). **B)** Phosphorylated (pS536) protein452 levels of the NF- $\kappa$ B p65 subunit in POVPC-treated c-Kit deficient, control, and c-Kit rescued453 SMC as determined by ELISA. Values are expressed as the mean  $\pm$  SD of the p-p65/total p65454 ratio normalized with respect to the control group ( $Kit^{+/+}$ ) (n=3 independent experiments). **C)**455 Protein expression of the NF- $\kappa$ B related pro-inflammatory mediators MMP-2 and MCP-1 in

456 POVPC-treated c-Kit deficient, control, and c-Kit rescued SMC as determined by Western blot.

457 Molecular weight markers are shown on the right side of the gel. Protein expression is expressed  
458 as the mean  $\pm$  SD of the MMP-2/ $\beta$ -actin and MCP-1/ $\beta$ -actin signal ratios normalized with  
459 respect to the control group (Kit<sup>+/+</sup>) (n=3 per cell type). \* p<0.05 and \*\* p<0.01 using a one-way  
460 ANOVA followed by a Newman-Keuls test.

461 **Figure 3. c-Kit inhibits NF- $\kappa$ B activity in smooth muscle cells (SMC) through the actions of**

462 **TAK1 and NLK. A)** Protein expression of the TAK1 and NLK regulatory proteins in c-Kit  
463 deficient (Kit<sup>W/W-v</sup>), control (Kit<sup>+/+</sup>), and c-Kit rescued SMC (Kit<sup>R</sup>) as determined by Western  
464 blot. Protein expression is expressed as the mean  $\pm$  standard deviation (SD) of the TAK1/ $\beta$ -actin  
465 and NLK/ $\beta$ -actin signal ratios normalized with respect to the control group (Kit<sup>+/+</sup>) (n=3 per cell  
466 type). **B-C)** Protein expression of TAK1 (**B**) and NLK (**C**) in Kit<sup>+/+</sup> cells transduced with  
467 lentivirus-encoded siRNAs of the corresponding targets or GFP control. Protein expression is  
468 expressed as the mean  $\pm$  SD of the TAK1/ $\beta$ -actin and NLK/ $\beta$ -actin signal ratios normalized with  
469 respect to the siGFP-treated group (n=3 independent experiments). **D)** NF- $\kappa$ B transcriptional  
470 activity in Kit<sup>+/+</sup> SMC transduced with lentivirus-encoded siRNAs complementary to TAK1,  
471 NLK, or GFP after 24-hour treatment with POVPC (50  $\mu$ g/ml), as determined by dual-luciferase  
472 assay. Transcriptional activity is represented as the mean  $\pm$  SD of the Firefly/Renilla luciferase  
473 ratio normalized with respect to the siGFP-treated group (n=3 independent experiments). **E)**  
474 Phosphorylated (pS536) protein levels of NF- $\kappa$ B p65 in POVPC-treated Kit<sup>+/+</sup> SMC transduced  
475 with lentivirus-encoded siRNAs as determined by ELISA. Values are expressed as the mean  $\pm$   
476 SD of the p-p65/total p65 ratio normalized with respect to the siGFP-treated group (n=3  
477 independent experiments). **F)** Protein expression of the pro-inflammatory mediators MMP-2 and  
478 MCP-1 in POVPC-treated Kit<sup>+/+</sup> SMC transduced with lentivirus-encoded siRNAs as determined  
479 by Western blot. Protein expression is expressed as the mean  $\pm$  SD of the MMP-2/ $\beta$ -actin and

480 MCP-1/ $\beta$ -actin signal ratios normalized with respect to the siGFP-treated group (n=3  
481 independent experiments). Molecular weight markers are shown on the right side of the gels. \*  
482  $p < 0.05$  and \*\*  $p < 0.01$  using a one-way ANOVA followed by a Newman-Keuls test.

483 **Figure 4. c-Kit forms a molecular complex with the regulatory proteins TAK1, Src, and**  
484 **NLK in smooth muscle cells (SMC).** **A)** Diagram illustrating the proposed molecular complex  
485 between c-Kit, TAK1, Src, and NLK in SMC and their inhibitory function on NF- $\kappa$ B regulated  
486 transcriptional activity. **B-C)** Co-immunoprecipitation experiments in control (Kit<sup>+/+</sup>) and c-Kit  
487 deficient (Kit<sup>W/W<sup>v</sup></sup>) SMC using anti-c-Kit (**B**) and anti-TAK1 antibodies (**C**) to pull down protein  
488 complexes. Molecular weight markers are shown on the right side of the gels, while antibodies  
489 used to detect eluted proteins are indicated on the left. IP, immunoprecipitation; IB, immunoblot.

490

491

492

493

494

495

496

497

498

499

## 500 REFERENCES

- 501 Ajibade, AA, Q Wang, J Cui, J Zou, X Xia, M Wang, Y Tong, W Hui, D Liu, B Su, HY Wang  
502 and RF Wang. 2012. Tak1 negatively regulates nf-kappab and p38 map kinase activation  
503 in gr-1+cd11b+ neutrophils. *Immunity* 36: 43-54.
- 504 Archer, SL. 1996. Diversity of phenotype and function of vascular smooth muscle cells. *J Lab*  
505 *Clin Med* 127: 524-529.
- 506 Bengatta, S, C Arnould, E Letavernier, M Monge, HM de Preneuf, Z Werb, P Ronco and B  
507 Lelongt. 2009. Mmp9 and scf protect from apoptosis in acute kidney injury. *J Am Soc*  
508 *Nephrol* 20: 787-797.
- 509 Bernstein, A, B Chabot, P Dubreuil, A Reith, K Nocka, S Majumder, P Ray and P Besmer. 1990.  
510 The mouse w/c-kit locus. *Ciba Found Symp* 148: 158-166; discussion 166-172.
- 511 Bernstein, A, L Forrester, AD Reith, P Dubreuil and R Rottapel. 1991. The murine w/c-kit and  
512 steel loci and the control of hematopoiesis. *Semin Hematol* 28: 138-142.
- 513 Chan, A, DL Newman, AM Shon, DH Schneider, S Kuldaneck and C Ober. 2006. Variation in the  
514 type i interferon gene cluster on 9p21 influences susceptibility to asthma and atopy.  
515 *Genes Immun* 7: 169-178.
- 516 Cheng, SL, JS Shao, LR Halstead, K Distelhorst, O Sierra and DA Towler. 2010. Activation of  
517 vascular smooth muscle parathyroid hormone receptor inhibits wnt/beta-catenin signaling  
518 and aortic fibrosis in diabetic arteriosclerosis. *Circ Res* 107: 271-282.
- 519 Clee, SM, N Bissada, F Miao, L Miao, AD Marais, HE Henderson, P Steures, J McManus, B  
520 McManus, RC LeBoeuf, JJ Kastelein and MR Hayden. 2000. Plasma and vessel wall  
521 lipoprotein lipase have different roles in atherosclerosis. *J Lipid Res* 41: 521-531.
- 522 Croft, M. 2009. The role of tnf superfamily members in t-cell function and diseases. *Nat Rev*  
523 *Immunol* 9: 271-285.
- 524 Damrauer, SM, CR Peterson, C Eva, P Studer and C Ferran. 2010. Partial loss of a20 (tnfaip3)  
525 promotes resistance to abdominal aortic aneurysms through altering smooth muscle cell  
526 differentiation. *Journal of the American College of Surgeons* 211: S137.
- 527 Davis, BN, AC Hilyard, PH Nguyen, G Lagna and A Hata. 2009. Induction of microrna-221 by  
528 platelet-derived growth factor signaling is critical for modulation of vascular smooth  
529 muscle phenotype. *J Biol Chem* 284: 3728-3738.
- 530 De Martin, R, M Hoeth, R Hofer-Warbinek and JA Schmid. 2000. The transcription factor nf-  
531 kappa b and the regulation of vascular cell function. *Arterioscler Thromb Vasc Biol* 20:  
532 E83-88.
- 533 Deng, L, L Huang, Y Sun, JM Heath, H Wu and Y Chen. 2015. Inhibition of foxo1/3 promotes  
534 vascular calcification. *Arterioscler Thromb Vasc Biol* 35: 175-183.
- 535 Drube, S, F Weber, C Gopfert, R Loschinski, M Rothe, F Boelke, MA Diamanti, T Lohn, J Ruth,  
536 D Schutz, N Hafner, FR Greten, R Stumm, K Hartmann, OH Kramer, A Dudeck and T  
537 Kamradt. 2015. Tak1 and ikk2, novel mediators of scf-induced signaling and potential  
538 targets for c-kit-driven diseases. *Oncotarget* 6: 28833-28850.
- 539 Giordano, M, R Roncagalli, P Bourdely, L Chasson, M Buferne, S Yamasaki, R Beyaert, G van  
540 Loo, N Auphan-Anezin, AM Schmitt-Verhulst and G Verdeil. 2014. The tumor necrosis  
541 factor alpha-induced protein 3 (tnfaip3, a20) imposes a brake on antitumor activity of cd8  
542 t cells. *Proc Natl Acad Sci U S A* 111: 11115-11120.

- 543 Hisamatsu, D, M Ohno-Oishi, S Nakamura, Y Mabuchi and H Naka-Kaneda. 2016. Growth  
544 differentiation factor 6 derived from mesenchymal stem/stromal cells reduces age-related  
545 functional deterioration in multiple tissues. *Aging (Albany NY)* 8: 1259-1275.
- 546 Hollenbeck, ST, K Sakakibara, PL Faries, B Workhu, B Liu and KC Kent. 2004. Stem cell factor  
547 and c-kit are expressed by and may affect vascular smcs through an autocrine pathway. *J*  
548 *Surg Res* 120: 288-294.
- 549 Huang, K, ZQ Yan, D Zhao, SG Chen, LZ Gao, P Zhang, BR Shen, HC Han, YX Qi and ZL  
550 Jiang. 2015. Sirt1 and foxo mediate contractile differentiation of vascular smooth muscle  
551 cells under cyclic stretch. *Cell Physiol Biochem* 37: 1817-1829.
- 552 Im, JE, SH Song and W Suh. 2016. Src tyrosine kinase regulates the stem cell factor-induced  
553 breakdown of the blood-retinal barrier. *Mol Vis* 22: 1213-1220.
- 554 Israel, A. 2010. The ikk complex, a central regulator of nf-kappab activation. *Cold Spring Harb*  
555 *Perspect Biol* 2: a000158.
- 556 Jin, QH, HX Shen, H Wang, QY Shou and Q Liu. 2013. Curcumin improves expression of scf/c-  
557 kit through attenuating oxidative stress and nf-kappab activation in gastric tissues of  
558 diabetic gastroparesis rats. *Diabetol Metab Syndr* 5: 12.
- 559 Karin, M. 1999. How nf-kappab is activated: The role of the ikappab kinase (ikk) complex.  
560 *Oncogene* 18: 6867-6874.
- 561 Kim, JY, JS Choi, SH Song, JE Im, JM Kim, K Kim, S Kwon, HK Shin, CK Joo, BH Lee and W  
562 Suh. 2014. Stem cell factor is a potent endothelial permeability factor. *Arterioscler*  
563 *Thromb Vasc Biol* 34: 1459-1467.
- 564 Klein, G, O Schmal and WK Aicher. 2015. Matrix metalloproteinases in stem cell mobilization.  
565 *Matrix Biol* 44-46: 175-183.
- 566 Kota, RS, CV Ramana, FA Tenorio, RI Enelow and JC Rutledge. 2005. Differential effects of  
567 lipoprotein lipase on tumor necrosis factor-alpha and interferon-gamma-mediated gene  
568 expression in human endothelial cells. *J Biol Chem* 280: 31076-31084.
- 569 Kumar, A and AM Boriek. 2003. Mechanical stress activates the nuclear factor-kappab pathway  
570 in skeletal muscle fibers: A possible role in duchenne muscular dystrophy. *FASEB J* 17:  
571 386-396.
- 572 Lawrence, T. 2009. The nuclear factor nf-kappab pathway in inflammation. *Cold Spring Harb*  
573 *Perspect Biol* 1: a001651.
- 574 Lee, SJ, KW Seo, MR Yun, SS Bae, WS Lee, KW Hong and CD Kim. 2008. 4-hydroxynonenal  
575 enhances mmp-2 production in vascular smooth muscle cells via mitochondrial ros-  
576 mediated activation of the akt/nf-kappab signaling pathways. *Free Radic Biol Med* 45:  
577 1487-1492.
- 578 Lennartsson, J and L Ronnstrand. 2006. The stem cell factor receptor/c-kit as a drug target in  
579 cancer. *Curr Cancer Drug Targets* 6: 65-75.
- 580 Lennartsson, J and L Ronnstrand. 2012. Stem cell factor receptor/c-kit: From basic science to  
581 clinical implications. *Physiol Rev* 92: 1619-1649.
- 582 Li, SZ, HH Zhang, JB Liang, Y Song, BX Jin, NN Xing, GC Fan, RL Du and XD Zhang. 2014.  
583 Nemo-like kinase (nlk) negatively regulates nf-kappa b activity through disrupting the  
584 interaction of tak1 with ikkbeta. *Biochim Biophys Acta* 1843: 1365-1372.
- 585 Livak, KJ and TD Schmittgen. 2001. Analysis of relative gene expression data using real-time  
586 quantitative pcr and the 2(-delta delta c(t)) method. *Methods* 25: 402-408.
- 587 Lu, Y, L Zhang, X Liao, P Sangwung, DA Prosdocimo, G Zhou, AR Votruba, L Brian, YJ Han,  
588 H Gao, Y Wang, K Shimizu, K Weinert-Stein, M Khrestian, DI Simon, NJ Freedman and

- 589 MK Jain. 2013. Kruppel-like factor 15 is critical for vascular inflammation. *J Clin Invest*  
590 123: 4232-4241.
- 591 Mack, CP. 2011. Signaling mechanisms that regulate smooth muscle cell differentiation.  
592 *Arterioscler Thromb Vasc Biol* 31: 1495-1505.
- 593 Matsui, J, T Wakabayashi, M Asada, K Yoshimatsu and M Okada. 2004. Stem cell factor/c-kit  
594 signaling promotes the survival, migration, and capillary tube formation of human  
595 umbilical vein endothelial cells. *J Biol Chem* 279: 18600-18607.
- 596 Maziere, C, M Auclair, M Djavaheri-Mergny, L Packer and JC Maziere. 1996. Oxidized low  
597 density lipoprotein induces activation of the transcription factor nf kappa b in fibroblasts,  
598 endothelial and smooth muscle cells. *Biochem Mol Biol Int* 39: 1201-1207.
- 599 Mehrhof, FB, R Schmidt-Ullrich, R Dietz and C Scheidereit. 2005. Regulation of vascular  
600 smooth muscle cell proliferation: Role of nf-kappab revisited. *Circ Res* 96: 958-964.
- 601 Metz, RP, JL Patterson and E Wilson. 2012. Vascular smooth muscle cells: Isolation, culture,  
602 and characterization. *Methods Mol Biol* 843: 169-176.
- 603 Micheva-Viteva, SN, Y Shou, KL Nowak-Lovato, KD Rector and E Hong-Geller. 2013. C-kit  
604 signaling is targeted by pathogenic yersinia to suppress the host immune response. *BMC*  
605 *Microbiol* 13: 249.
- 606 Miyamoto, T, Y Sasaguri, T Sasaguri, S Azakami, H Yasukawa, S Kato, N Arima, K Sugama  
607 and M Morimatsu. 1997. Expression of stem cell factor in human aortic endothelial and  
608 smooth muscle cells. *Atherosclerosis* 129: 207-213.
- 609 Miyazawa, K, DA Williams, A Gotoh, J Nishimaki, HE Broxmeyer and K Toyama. 1995.  
610 Membrane-bound steel factor induces more persistent tyrosine kinase activation and  
611 longer life span of c-kit gene-encoded protein than its soluble form. *Blood* 85: 641-649.
- 612 Montani, D, F Perros, N Gambaryan, B Girerd, P Dorfmueller, LC Price, A Huertas, H Hammad,  
613 B Lambrecht, G Simonneau, JM Launay, S Cohen-Kaminsky and M Humbert. 2011. C-  
614 kit-positive cells accumulate in remodeled vessels of idiopathic pulmonary arterial  
615 hypertension. *Am J Respir Crit Care Med* 184: 116-123.
- 616 Ogbozor, UD, M Opene, LS Renteria, S McBride and BO Ibe. 2015. Mechanism by which  
617 nuclear factor-kappa beta (nf-kb) regulates ovine fetal pulmonary vascular smooth  
618 muscle cell proliferation. *Mol Genet Metab Rep* 4: 11-18.
- 619 Patel, VI, S Daniel, CR Longo, GV Shrikhande, ST Scali, E Czismadia, CM Groft, T Shukri, C  
620 Motley-Dore, HE Ramsey, MD Fisher, ST Grey, MB Arvelo and C Ferran. 2006. A20, a  
621 modulator of smooth muscle cell proliferation and apoptosis, prevents and induces  
622 regression of neointimal hyperplasia. *FASEB J* 20: 1418-1430.
- 623 Pegorier, S, D Stengel, H Durand, M Croset and E Ninio. 2006. Oxidized phospholipid: Povpc  
624 binds to platelet-activating-factor receptor on human macrophages. Implications in  
625 atherosclerosis. *Atherosclerosis* 188: 433-443.
- 626 Pidkovka, NA, OA Cherepanova, T Yoshida, MR Alexander, RA Deaton, JA Thomas, N  
627 Leitinger and GK Owens. 2007. Oxidized phospholipids induce phenotypic switching of  
628 vascular smooth muscle cells in vivo and in vitro. *Circ Res* 101: 792-801.
- 629 Ramana, KV, B Friedrich, S Srivastava, A Bhatnagar and SK Srivastava. 2004. Activation of  
630 nuclear factor-kappab by hyperglycemia in vascular smooth muscle cells is regulated by  
631 aldose reductase. *Diabetes* 53: 2910-2920.
- 632 Savai, R, HM Al-Tamari, D Sedding, B Kojonazarov, C Muecke, R Teske, MR Capecchi, N  
633 Weissmann, F Grimminger, W Seeger, RT Schermuly and SS Pullamsetti. 2014. Pro-

- 634 proliferative and inflammatory signaling converge on foxo1 transcription factor in  
635 pulmonary hypertension. *Nat Med* 20: 1289-1300.
- 636 Skartsis, N, L Martinez, JC Duque, M Tabbara, OC Velazquez, A Asif, F Andreopoulos, LH  
637 Salman and RI Vazquez-Padron. 2014. C-kit signaling determines neointimal hyperplasia  
638 in arteriovenous fistulae. *Am J Physiol Renal Physiol* 307: F1095-1104.
- 639 Song, L, C Kang, Y Sun, W Huang, W Liu and Z Qian. 2016. Crocetin inhibits  
640 lipopolysaccharide-induced inflammatory response in human umbilical vein endothelial  
641 cells. *Cell Physiol Biochem* 40: 443-452.
- 642 Song, L, G Selman, N Santos, L Martinez, RM Lassance-Soares, K Webster and RI Vazquez-  
643 Padron. 2016. C-kit expression in vascular smooth muscle cells protects mice against  
644 excessive atherosclerosis. *Circulation* 134: A14889.
- 645 Sukhanov, S, Y Higashi, SY Shai, C Vaughn, J Mohler, Y Li, YH Song, J Titterington and P  
646 Delafontaine. 2007. Igf-1 reduces inflammatory responses, suppresses oxidative stress,  
647 and decreases atherosclerosis progression in apoe-deficient mice. *Arterioscler Thromb*  
648 *Vasc Biol* 27: 2684-2690.
- 649 Tang, RH, XL Zheng, TE Callis, WE Stansfield, J He, AS Baldwin, DZ Wang and CH Selzman.  
650 2008. Myocardin inhibits cellular proliferation by inhibiting nf-kappab(p65)-dependent  
651 cell cycle progression. *Proc Natl Acad Sci U S A* 105: 3362-3367.
- 652 Vladykovskaya, E, E Ozhegov, JD Hoetker, Z Xie, Y Ahmed, J Suttles, S Srivastava, A  
653 Bhatnagar and OA Barski. 2011. Reductive metabolism increases the proinflammatory  
654 activity of aldehyde phospholipids. *J Lipid Res* 52: 2209-2225.
- 655 Wang, CH, N Anderson, SH Li, PE Szmítko, WJ Cherng, PW Fedak, S Fazel, RK Li, TM Yau,  
656 RD Weisel, WL Stanford and S Verma. 2006. Stem cell factor deficiency is  
657 vasculoprotective: Unraveling a new therapeutic potential of imatinib mesylate. *Circ Res*  
658 99: 617-625.
- 659 Wang, CH, S Verma, IC Hsieh, A Hung, TT Cheng, SY Wang, YC Liu, WL Stanford, RD  
660 Weisel, RK Li and WJ Cherng. 2007. Stem cell factor attenuates vascular smooth muscle  
661 apoptosis and increases intimal hyperplasia after vascular injury. *Arterioscler Thromb*  
662 *Vasc Biol* 27: 540-547.
- 663 Yang, J, H Jiang, SS Chen, J Chen, SK Xu, WQ Li and JC Wang. 2010. Cbp knockdown inhibits  
664 angiotensin ii-induced vascular smooth muscle cells proliferation through downregulating  
665 nf-kb transcriptional activity. *Mol Cell Biochem* 340: 55-62.
- 666 Yasuda, J, H Yokoo, T Yamada, I Kitabayashi, T Sekiya and H Ichikawa. 2004. Nemo-like  
667 kinase suppresses a wide range of transcription factors, including nuclear factor-kappab.  
668 *Cancer Sci* 95: 52-57.
- 669 Yoshida, T and GK Owens. 2005. Molecular determinants of vascular smooth muscle cell  
670 diversity. *Circ Res* 96: 280-291.
- 671 Young, KC, E Torres, D Hehre, S Wu, C Suguihara and JM Hare. 2016. Antagonism of stem cell  
672 factor/c-kit signaling attenuates neonatal chronic hypoxia-induced pulmonary vascular  
673 remodeling. *Pediatr Res* 79: 637-646.
- 674 Zahradka, P, JP Werner, S Buhay, B Litchie, G Helwer and S Thomas. 2002. Nf-kappab  
675 activation is essential for angiotensin ii-dependent proliferation and migration of vascular  
676 smooth muscle cells. *J Mol Cell Cardiol* 34: 1609-1621.
- 677 Zakiryanova, G, O Karpova, O Khamdiyeva, D Kopytina, N Urazalieva, E Kustova and Z  
678 Biyasheva. 2014. C-kit/scf autocrine loop in human nk cells (ccr5p.254). *J Immunol* 192:  
679 181.188.

- 680 Zhao, G, L Shi, D Qiu, H Hu and PN Kao. 2005. Nf45/ilf2 tissue expression, promoter analysis,  
681 and interleukin-2 transactivating function. *Exp Cell Res* 305: 312-323.
- 682 Ziouzenkova, O, S Perrey, L Asatryan, J Hwang, KL MacNaul, DE Moller, DJ Rader, A  
683 Sevanian, R Zechner, G Hoefler and J Plutzky. 2003. Lipolysis of triglyceride-rich  
684 lipoproteins generates ppar ligands: Evidence for an antiinflammatory role for lipoprotein  
685 lipase. *Proc Natl Acad Sci U S A* 100: 2730-2735.
- 686

**Table 1** (on next page)

Table 1. Selected list of differentially expressed genes in c-Kit deficient vs. wild type smooth muscle cells

**Table 1. List of select differentially expressed genes in c-Kit deficient vs. wild type smooth muscle cells**

Gene Symbol	Gene Product	Fold Change <sup>a</sup>	P-Value
<b>Transcription Factors</b>			
Crebbp	CREB binding protein	-1.18	0.010
Foxo1	Forkhead box O1	-2.05	0.007
Ilf2	Interleukin enhancer binding factor 2	1.38	0.034
Irf3	Interferon regulatory factor 3	-1.14	0.029
Nfatc1	Nuclear factor of activated T-cells 1	-1.36	0.040
Nfatc2	Nuclear factor of activated T-cells 2	2.01	0.033
Nfatc4	Nuclear factor of activated T-cells 4	-2.32	0.009
<b>Cell Adhesion Proteins</b>			
Cdh5	Cadherin 5	-5.00	0.043
Itga9	Integrin subunit alpha 9	-2.91	0.047
Itga11	Integrin subunit alpha 11	-13.28	0.034
Pcdh7	Protocadherin 7	-2.71	0.015
Pcdha1	Protocadherin alpha 1	-1.44	0.042
Pcdha8	Protocadherin alpha 8	2.26	0.002
Selp1g	P-selectin glycoprotein ligand 1	-3.94	0.006
<b>Cytokines/Growth Factors</b>			
Ccl6	Chemokine (C-C motif) ligand 6	-8.76	0.005
Gdf6	Growth differentiation factor 6	-4.10	0.019
Ifna14	Interferon alpha 14	1.27	0.043
Igf1	Insulin-like growth factor 1	-5.06	0.027
Pdgfb	Platelet-derived growth factor subunit B	-2.59	0.011
Pgf	Placental growth factor	-4.96	0.037
Tnfsf9	Tumor necrosis factor ligand superfamily member 9	2.97	0.048
<b>Enzymes</b>			
Bmp1	Bone morphogenetic protein 1	-2.36	0.016
Casp3	Caspase 3	2.06	0.040
Ccnd1	Cyclin D1	2.20	0.043
Gucylb3	Guanylate cyclase 1 soluble subunit beta	-8.95	0.033
Ikkbb	Inhibitor of nuclear factor kappa-B kinase subunit beta	1.34	0.001
Lpl	Lipoprotein lipase	-14.24	0.022
Mmp23	Matrix metalloproteinase 23	-6.61	0.049
Pde1a	Ca <sup>2+</sup> /calmodulin dependent phosphodiesterase 1A	-4.73	0.028
Pde2a	Phosphodiesterase 2A	-1.91	0.048
Prkg1	cGMP-dependent protein kinase 1 (PKG)	-9.09	0.034
Ptgs1	Prostaglandin-endoperoxide synthase 1 (COX-1)	2.22	0.027
Sirt1	Sirtuin 1	-1.52	0.034
Tnfaip3	TNF alpha induced protein 3	3.46	<0.001
<b>Receptors</b>			
Adra2a	Adrenoceptor alpha 2A	-6.49	0.002
Agtr1b	Angiotensin II type 1b receptor	-9.88	0.043
Avpr1a	Arginine vasopressin receptor 1A	-6.62	0.010
Cxcr4	Chemokine (C-X-C motif) receptor 4	-6.55	0.040
Igf2r	Insulin like growth factor 2 receptor	-1.48	0.012
Il3ra	Interleukin 3 receptor subunit alpha	-2.38	0.023
Il20ra	Interleukin 20 receptor alpha	-3.52	0.003
Pdgfrb	Platelet-derived growth factor receptor beta	-2.89	0.016
Pth1r	Parathyroid hormone 1 receptor	-5.42	0.002

<sup>a</sup> Average fold gene expression change in c-Kit deficient smooth muscle cells compared to wild type cells.

**Table 2** (on next page)

Table 2. Selected canonical pathways with differentially expressed genes in c-Kit deficient vs. wild type smooth muscle cells

**Table 2. Select canonical pathways with differentially expressed genes in c-Kit deficient vs. wild type smooth muscle cells**

Pathway	Biological Function	P-Value	Z-Score <sup>a</sup>	Predicted Status <sup>a</sup>	Differentially Expressed Genes
PTEN signaling <sup>b</sup>	Proliferation, apoptosis, de-differentiation, cell migration, inflammation	<0.001	0.258	Activation	Akt2, Casp3, Rac1, Ccnd1, Igf2r, Rac3, Ddr1, Shc1, Ikbkb, Inpp5f, Foxo1, Bmpr1a, Magi2, Magi3, Pdgfrb
Death receptor signaling <sup>b</sup>	Apoptosis	0.003	1.265	Activation	Map2k4, Gas2, Rock1, Diablo, Ikbkb, Casp3, Htra2, Tbk1, Parp1, Birc2
TNFR2 signaling <sup>b</sup>	Cell survival, inflammation	0.005	1.000	Activation	Map2k4, Ikbkb, Tnfaip3, Tbk1, Birc2
Wnt/ $\beta$ -catenin signaling	Proliferation, cell survival, cell migration	0.008	0.577	Activation	Sfrp4, Akt2, Crebbp, Csnk1a1, Fzd9, Ccnd1, Rarg, Fzd8, Cdh5, Dkk3, Sox18, Ppp2r5e, Sfrp1, Wnt5b
IRF activation pathway <sup>b</sup>	Inflammation	0.011	1.134	Activation	Map2k4, Ikbkb, Crebbp, Tbk1, Ifna14, Irf3, Atf2
ERK/MAPK signaling	Proliferation, cell migration, vasoconstriction	0.028	1.069	Activation	Crebbp, Rac1, Ppp1r14a, Mknk2, Rac3, Nfatc1, Atf2, Pla2g4e, Shc1, Pla2g6, Prkar2b, Prkag2, Rps6ka1, Ppp2r5e
TNFR1 signaling <sup>b</sup>	Cell survival, inflammation	0.044	1.000	Activation	Map2k4, Ikbkb, Casp3, Tnfaip3, Birc2
Wnt/ $Ca^{2+}$ pathway <sup>b</sup>	Proliferation, cell migration	<0.001	-1.000	Inhibition	Fzd8, Plcb4, Crebbp, Nfatc2, Fzd9, Nfatc4, Wnt5b, Nfatc1, Atf2
AMPK signaling <sup>b</sup>	Cellular senescence, anti-inflammatory, differentiation, vasoconstriction	<0.001	-0.535	Inhibition	Pbrm1, Akt2, Crebbp, Ccnd1, Slc2a4, Elavl1, Atf2, Ak6, Prkar2b, Foxo1, Adra2a, Ppm1b, Sirt1, Prkag2, Ppm1a, Ppp2r5e, Ppat, Camkk2
Apoptosis signaling <sup>b</sup>	Apoptosis	<0.001	-0.302	Inhibition	Map2k4, Gas2, Rock1, Diablo, Ikbkb, Casp3, Htra2, Rps6ka1, Bcl2a1, Parp1, Birc2
Phospholipase C signaling	Vasoconstriction, stress responses	0.001	-0.378	Inhibition	Rala, Arhgef12, Pld3, Fcgr2a, Arhgef15, Crebbp, Rac1, Ppp1r14a, Nfatc4, Fcgr2b, Rhoh, Nfatc1, Atf2, Pla2g6, Shc1, Pla2g4e, Plcb4, Itpr3, Fcer1g, Nfatc2
Nitric oxide/GC signaling	Vasodilation	0.005	-0.302	Inhibition	Bdkrb2, Kng1, Pde2a, Akt2, Prkg1, Prkar2b, Itpr3, Prkag2, Pde1a, Gucy1b3, Pgf
Integrin signaling	Cell adhesion, cell migration, proliferation, apoptosis, stress responses, differentiation	0.029	-1.387	Inhibition	Map2k4, Akt2, Rala, Rac1, Rac3, Rhoh, Pdgfb, Rock1, Arhgap5, Shc1, Itga11, Itga9, Actn4, Tspan6, Nedd9
Adipogenesis pathway	Lipid synthesis and storage	<0.001	N.D.	Could not be predicted	Nr2f2, Sin3b, Fzd9, Nfatc4, Rbp1, Slc2a4, Fzd8, Cdk5, Foxo1, Bmpr1a, Lpl, Sirt1, Ctbp2, Clock, Fabp4, Rps6ka1, Stat5b
Fibroblast inflammatory pathway <sup>b</sup>	Proliferation, cell migration, differentiation, inflammation	0.012	N.D.	Could not be predicted	Map2k4, Sfrp4, Akt2, Crebbp, Csnk1a1, Rac1, Fzd9, Nfatc4, Ccnd1, Nfatc1, Pdgfb, Pgf, Atf2, Rock1, Ikbkb, Fzd8, Plcb4, Dkk3, Nfatc2, Sfrp1, Wnt5b
Gaq signaling <sup>b</sup>	Proliferation, cell migration, vasoconstriction	0.026	0.000	Could not be predicted	Rock1, Ikbkb, Plcb4, Akt2, Pld3, Agtr1b, Itpr3, Nfatc2, Nfatc4, Avpr1a, Rhoh, Nfatc1

<sup>a</sup> Z-score and predicted functional status in c-Kit deficient smooth muscle cells compared to wild type cells. The z-score measures how well the gene expression data matches the experimentally observed direction of pathway regulation in the literature. A positive z-score predicts activation, while a negative z-score indicates inhibition. N.D., could not be determined.

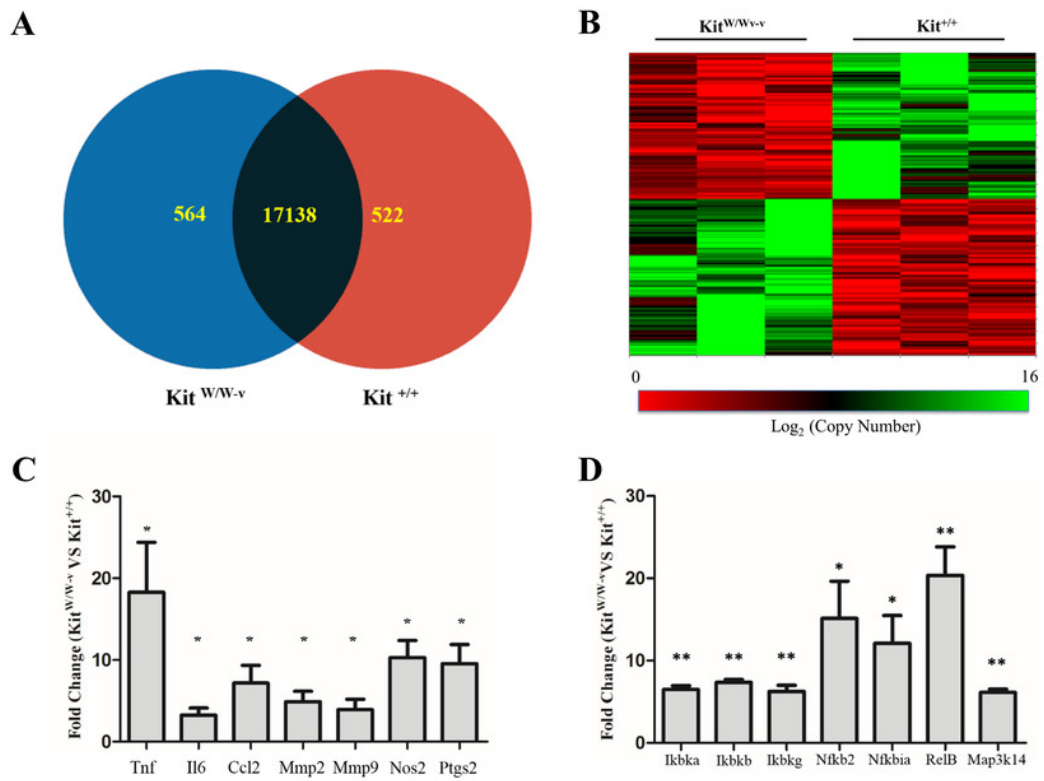
<sup>b</sup> NF- $\kappa$ B associated signaling pathway



# Figure 1

Figure 1. Loss of c-Kit function accounts for significant gene expression differences between c-Kit deficient and wild type smooth muscle cells (SMC).

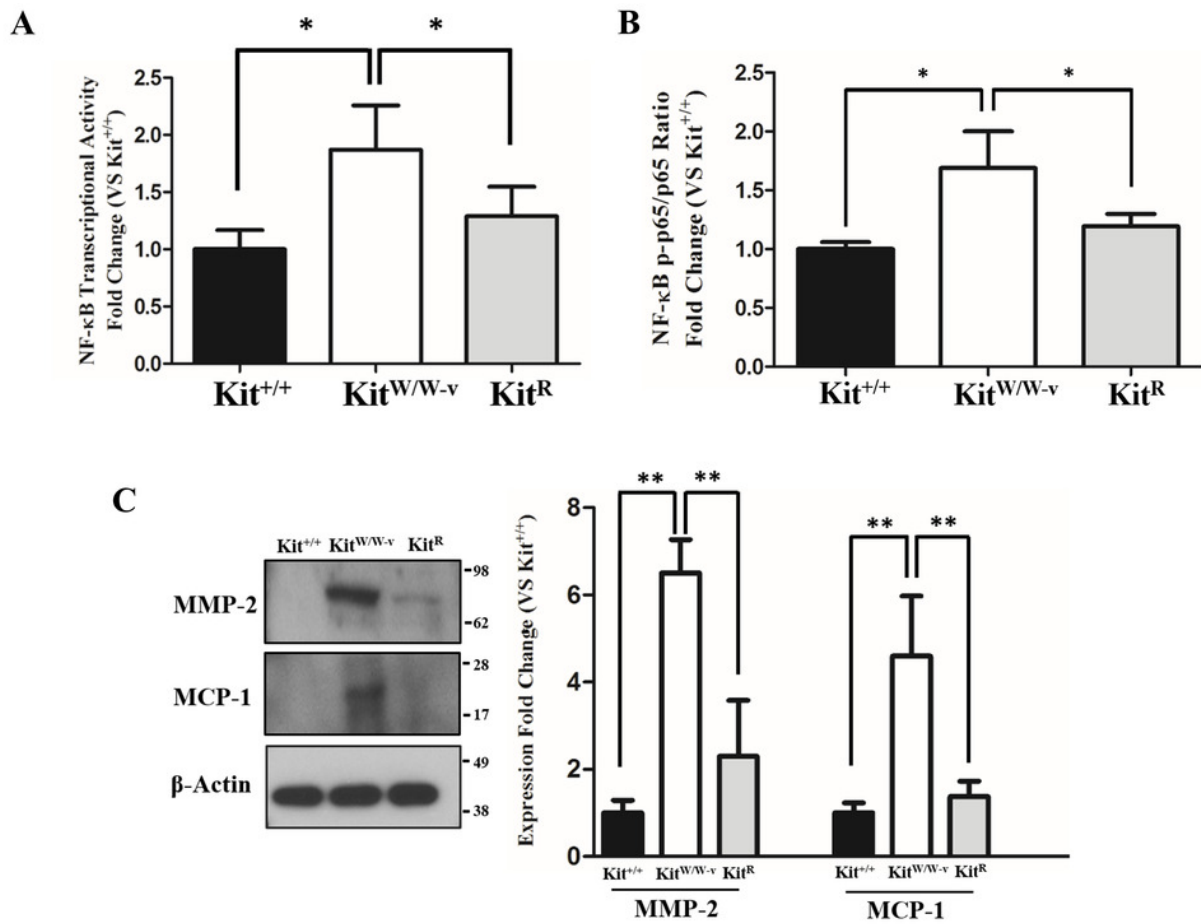
**A)** Venn diagram indicating the numbers of differentially upregulated genes in primary SMC isolated from c-Kit deficient (blue; Kit<sup>W/W-v</sup>) and littermate control mice (red; Kit<sup>+/+</sup>) as determined by microarray analysis. The group of genes in the interception (black area) did not show statistically significant differences by *t*-test between the two strains (n=3 per group). **B)** Heat map of differentially expressed genes in primary SMC from c-Kit deficient and littermate control mice. **C)** Expression of NF-κB related genes in c-Kit deficient vs. control SMC as determined by real-time PCR. Values are shown as fold change over expression in Kit<sup>+/+</sup> cells; \* p<0.05 and \*\* p<0.01 using a two-tailed *t*-test assuming unequal variance, n=3 per group.



## Figure 2

Figure 2. Loss of c-Kit function in primary smooth muscle cells (SMC) is associated with increased NF- $\kappa$ B activity.

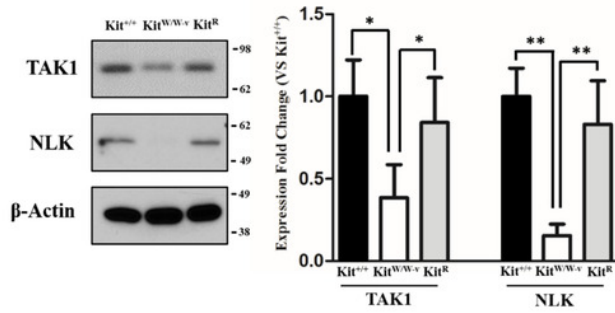
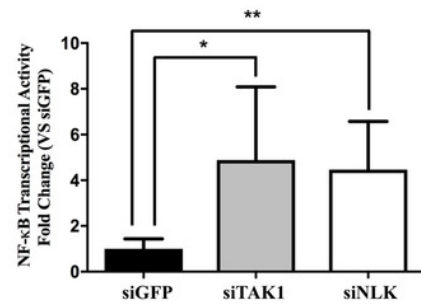
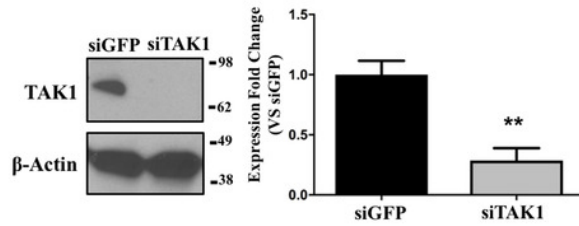
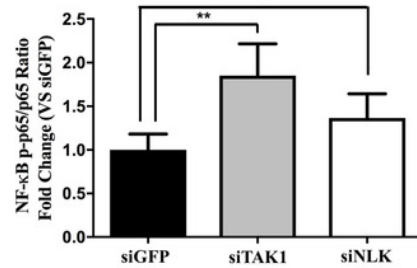
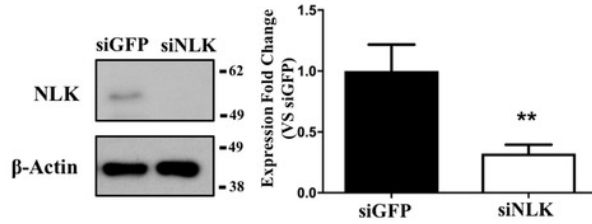
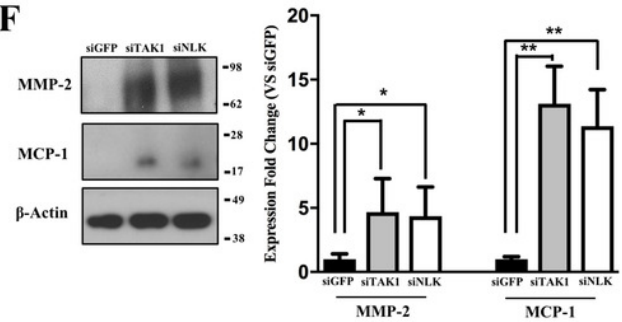
**A)** NF- $\kappa$ B transcriptional activity in c-Kit deficient ( $Kit^{W/W-v}$ ), control ( $Kit^{+/+}$ ), and c-Kit rescued SMC ( $Kit^R$ ) after 24-hour treatment with POVPC (50  $\mu$ g/ml), as determined by dual-luciferase reporter assay. Transcriptional activity is represented as the mean  $\pm$  standard deviation (SD) of the Firefly/Renilla luciferase ratio normalized with respect to the control group ( $Kit^{+/+}$ ) (n=3 independent experiments). **B)** Phosphorylated (pS536) protein levels of the NF- $\kappa$ B p65 subunit in POVPC-treated c-Kit deficient, control, and c-Kit rescued SMC as determined by ELISA. Values are expressed as the mean  $\pm$  SD of the p-p65/total p65 ratio normalized with respect to the control group ( $Kit^{+/+}$ ) (n=3 independent experiments). **C)** Protein expression of the NF- $\kappa$ B related pro-inflammatory mediators MMP-2 and MCP-1 in POVPC-treated c-Kit deficient, control, and c-Kit rescued SMC as determined by Western blot. Molecular weight markers are shown on the right side of the gel. Protein expression is expressed as the mean  $\pm$  SD of the MMP-2/ $\beta$ -actin and MCP-1/ $\beta$ -actin signal ratios normalized with respect to the control group ( $Kit^{+/+}$ ) (n=3 per cell type). \* p<0.05 and \*\* p<0.01 using a one-way ANOVA followed by a Newman-Keuls test.



## Figure 3

Figure 3. c-Kit inhibits NF- $\kappa$ B activity in smooth muscle cells (SMC) through the actions of TAK1 and NLK.

**A)** Protein expression of the TAK1 and NLK regulatory proteins in c-Kit deficient ( $\text{Kit}^{\text{W/W-v}}$ ), control ( $\text{Kit}^{+/+}$ ), and c-Kit rescued SMC ( $\text{Kit}^{\text{R}}$ ) as determined by Western blot. Protein expression is expressed as the mean  $\pm$  standard deviation (SD) of the TAK1/ $\beta$ -actin and NLK/ $\beta$ -actin signal ratios normalized with respect to the control group ( $\text{Kit}^{+/+}$ ) ( $n=3$  per cell type). **B-C)** Protein expression of TAK1 (**B**) and NLK (**C**) in  $\text{Kit}^{+/+}$  cells transduced with lentivirus-encoded siRNAs of the corresponding targets or GFP control. Protein expression is expressed as the mean  $\pm$  SD of the TAK1/ $\beta$ -actin and NLK/ $\beta$ -actin signal ratios normalized with respect to the siGFP-treated group ( $n=3$  independent experiments). **D)** NF- $\kappa$ B transcriptional activity in  $\text{Kit}^{+/+}$  SMC transduced with lentivirus-encoded siRNAs complementary to TAK1, NLK, or GFP after 24-hour treatment with POVPC (50  $\mu\text{g/ml}$ ), as determined by dual-luciferase assay. Transcriptional activity is represented as the mean  $\pm$  SD of the Firefly/Renilla luciferase ratio normalized with respect to the siGFP-treated group ( $n=3$  independent experiments). **E)** Phosphorylated (pS536) protein levels of NF- $\kappa$ B p65 in POVPC-treated  $\text{Kit}^{+/+}$  SMC transduced with lentivirus-encoded siRNAs as determined by ELISA. Values are expressed as the mean  $\pm$  SD of the p-p65/total p65 ratio normalized with respect to the siGFP-treated group ( $n=3$  independent experiments). **F)** Protein expression of the pro-inflammatory mediators MMP-2 and MCP-1 in POVPC-treated  $\text{Kit}^{+/+}$  SMC transduced with lentivirus-encoded siRNAs as determined by Western blot. Protein expression is expressed as the mean  $\pm$  SD of the MMP-2/ $\beta$ -actin and MCP-1/ $\beta$ -actin signal ratios normalized with respect to the siGFP-treated group ( $n=3$  independent experiments). Molecular weight markers are shown on the right side of the gels. \*  $p<0.05$  and \*\*  $p<0.01$  using a one-way ANOVA followed by a Newman-Keuls test.

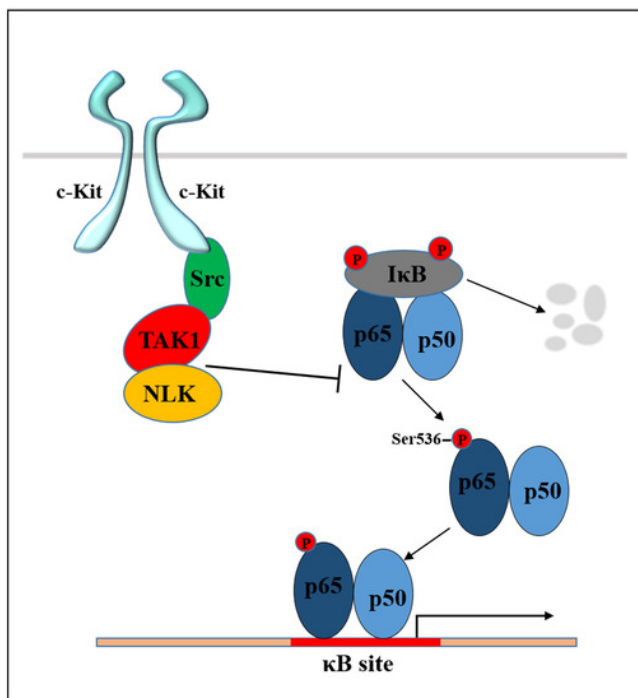
**A****D****B****E****C****F**

## Figure 4

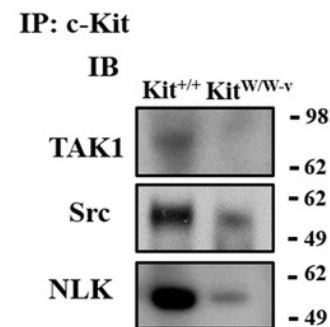
Figure 4. c-Kit forms a molecular complex with the regulatory proteins TAK1, Src, and NLK in smooth muscle cells (SMC).

**A)** Diagram illustrating the proposed molecular complex between c-Kit, TAK1, Src, and NLK in SMC and their inhibitory function on NF- $\kappa$ B transcriptional activity. **B-C)** Co-immunoprecipitation experiments in control (Kit<sup>+/+</sup>) and c-Kit deficient (Kit<sup>W/W-v</sup>) SMC using anti-c-Kit (**B**) and anti-TAK1 antibodies (**C**) to pull down protein complexes. Molecular weight markers are shown on the right side of the gels, while antibodies used to detect eluted proteins are indicated on the left. IP, immunoprecipitation; IB, immunoblot.

**A**



**B**



**C**

